20

Bonded Composite Patch Repairs on Cracked Aluminum Plates: Theory, Modeling and Experiments

Fabrizio Ricci, Francesco Franco and Nicola Montefusco
University of Naples "Federico II", Department of Aerospace Engineering
Italy

1. Introduction

Composite patches, bonded on cracked or corroded metallic aircraft structures, have shown to be a highly cost effective method for extending the service life and maintaining high structural efficiency (Baker & Jones, 1988; Baker, 1993; Molent et al., 1989; Baker et al., 1984; Torkington, 1991; Bartholomeus, 1991).

Damage tolerant and fail-safe design of aircraft, aerospace and civil structures requires a substantial amount of inspection and defects-monitoring at regular intervals. There is a large number of high-cost inventory of aircraft structures in operation throughout Europe and the world, that are undergoing continuous degradation through aging. Moreover, this number is increasing by around 5% every year, resulting in significant negative impact on the economy of many nations. The degradation of defects critical structures is controlled through careful and expensive regularly scheduled inspections in an effort to reduce their risk of failure.

The replacement of a damaged structural component has a relevant impact on the life cycle cost of an airplane. Bonded composite patches for repairing cracks and defects in aircraft structures have been widely used in the last years. This technology offers many advantages over mechanical fastening or riveting, including improved fatigue behavior, restored stiffness and strength, reduced corrosion and readily formed into complex shapes. The repair of metal structures with composite materials is a technology that was first introduced in Australia in the early 1970s and later in USA in early 1980s. It is now estimated that over 10 000 flying patch repairs, for corrosion and fatigue damages, have been performed on Australian and US military aircraft (Christian et al., 1992; Umamaheswar & Singh, 1999; Roach, 1995). This technology was first used for the repair of military aircraft and then applied also to civil aircraft. The success of a bonding repair depends on the properties of both the adhesive and the patch. The quality of the repair depends upon bonding process and surface treatment as well. Carbon–epoxy composites have been mostly used in aeronautics due to their high stiffness and strength to weight ratios. The performance of the adhesive plays a key role in the successful utilization of bonded composite patch repairs.

The role of a bonded composite patch is to restore the stress state modified by the presence of the crack. The stress intensity factor is then reduced by the presence of the patch. Many authors have already investigated the behavior of metallic structures repaired by composite

patches. Baker and Jones (Baker & Jones, 1988) studied an aluminum panel repaired with composite patches. For a repaired cracked plate they showed that the stress intensity factor does not increase indefinitely with the crack length, as it asymptotically reaches a limit value. According to Baker's results, Rose (Rose, 1981 and 1982) showed that the stress intensity factor range of a repaired structure does not depend on the crack length if the crack grows up below the repair. As a result, the crack growth rate does not depend on of crack length according to the Paris law. Klug (Klug et al., 1999) investigated the fatigue behaviour of pre-cracked 2024-T3 aluminum plates repaired with a bonded carbon/epoxy patch. Single sided repairs were found to provide about a 4-5 times improvement in the fatigue life.

After these early works many authors have addressed many numerical and experimental aspects. Naboulsi, Schubbe and Mall (Nabulosi & Mall, 1996; Schubbe & Mall, 1999) have analyzed the modeling of the composite and adhesive layers, using the three layer technique in comparison with the high computational cost of the three dimensional Finite Element models. Naboulsi and Mall (Nabulosi & Mall, 1998) have successively adopted the three layer technique for the nonlinear analysis of the repaired structure in order to take in account large displacements and material nonlinearities. Chung and Yang (Chung & Yang, 2002) and Jones, Whittingham and Marshall (Jones et al., 2002) have investigated the fracture and the crack growth behavior in a more complex structure, such as stiffened panel, deriving some design formulas. Tong and Sun (Tong and Sun, 2003) have presented a novel finite element formulation for developing adhesive elements and conducting a simplified non-linear stress analysis of bonded repairs in curved structures. Some other authors have focused their attention on the optimal design of the bonded patches, by finite element models, in terms of edge taper (Wang et al., 2005) and in-plane shape (Mahadesh & Hakeem, 2000).

Some of the above mentioned numerical activities have been compared with experimental data measured with reference to the stress intensity factor and fatigue life of the repaired structural elements (Schubbe & Mall, 1999; Wang et al., 2005;).

The aim of this work is to review the capability of finite element models in estimating the mechanical behavior of metallic panels repaired by composite patches. The attention has been focused on those commercial codes implementing the "quarter-point location" formulation. The interest in commercial finite element codes is due to their use in most of the industrial applications. Furthermore the validation of the finite element procedures for a metallic panel with a composite patch repair is a promising result for the analysis of composite structures to be repaired with composite patches.

The numerical analyses, limited to the case of mode I (opening crack), have been strongly supported by well known theoretical formulations and several experimental tests. Moreover, the experimental data allowed a comparison among different patches, adhesives and surface preparation properties.

In this work a repair with a single patch - single sided configuration - (i.e. bonded only on one side of the panel) has been considered. This configuration could avoid the removal of the damaged component and in general could lead to a significant reduction of time and costs of repair operations.

Section 2 of the paper presents the geometry of the panel used as test-case. Section 3 reviews the mechanical behavior of the cracked panel. The mechanical behavior of the repaired panel, estimated by the numerical models, is presented in Section 4 and the comparison with the experimental data is discussed in Section 5. Finally, Section 6 summarizes the work conclusions and outlines some final considerations.

1.1 List of symbols

a	Half crack length – total crack length: 2a
BC	correction term
C	material constants
E	Young's modulus
G	shear modulus
G_I	energy release rate
H	Patch length
K_I	stress intensity factor, elastic
I	moment of inertia
K_I^*	stress intensity factor, elasto-plastic
K_{IC}	fracture toughness
K_R	stress intensity factor for a one sided repair
K_{th}	threshold value
m	material constants
N	number of cycles
r_y	plastic radius
t	Thickness
U	elastic strain energy
W	plate width
Y	geometry factor
y_{max}	distance of the extreme fiber ply from the neutral axis

Greek symbols

β	shear stress transfer length
υ	Poisson's ratio
σ	asymptotic stress
σ_s	yield strength
σ_{max}	asymptotic stress max
σ_{min}	asymptotic stress min
σ_o	nominal stress
$\Delta K=K_{max}-K_{min}$	Stress intensity range
$\Delta\sigma = \sigma_{max} - \sigma_{min}$	Stress range

Notations

a	adhesive subscript
p	plate subscript
r	patch subscript

2. Panel geometry

The geometry of the cracked structure in the present work is shown in Fig. 1. It was considered a 6061–T6 aluminum alloy plate; a through thickness crack is used to simulate the defect in the structural components.

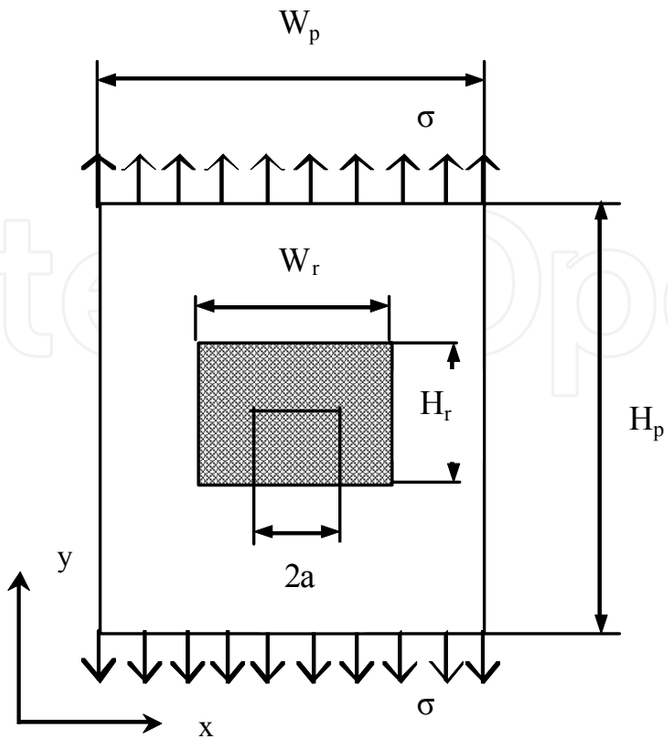

Fig. 1. The geometry of panel with the patch

The fracture is made with the technique of Electrical Discharge Machining (EDM), based on the erosion of metals by spark discharges. This technique allows an accurate control of the crack size and tips shape. The size of the panel is: *Hp* = 180 [mm], *Wp* = 180 [mm] and thickness *tp* = 1.5 [mm]. The central crack has a length *2a* = 40 [mm] repaired by carbon-epoxy composite patch bonded with adhesive having an estimated thickness *ta* = 0.1 [mm]. Tables 1 and 2 show the mechanical properties of the patch and adhesives used. The height and width of the patch are *Hr* = 40 [mm] and *Wr* = 60 [mm], respectively. It is well known (Mahadesh & Hakeem, 2000) that the rectangular shape of the patch is not the best choice; nevertheless the rectangular shape is a good compromise between mechanical performances and manufacturing aspects. The patch size is the result of various numerical tests not reported here for the sake of brevity. It represents the minimum patch size, covering integrally the crack length, that leads to a significant improvement of the mechanical behavior under the considered loading conditions as shown in the next Sections.

	Type 1	**Type 2**
E_r [GPa]	18.00	12.73
G_r [Gpa]	34.90	24.76
υ_r	0.68	0.7
ply orientation	[45/-45]	[(45)]Fabric
t_r [mm]	0.6	0.3

Table 1. Patch properties

Two types of carbon-epoxy patches were used. Type 1 is a two unidirectional layers +45°/-45° patch, and Type 2 is a single fabric layer patch with the fibers oriented along the ± 45° directions.

	Loctite Hysol EA95	**Cytec FM73**	**AF163-2K**
E_a [GPa]	2.48	1.43	1.10
G_a [Gpa]	0.905	0.53	0.44
υ_a	0.37	0.35	0.34
t_a [mm]	0.1	0.1	0.1

Table 2. Adhesive properties

E [GPa]	68.00
G [GPa]	26.20
υ_r	0.33
σ_s [MPa]	276
K_{IC} [MPa√m]	28.57
K_{IC} [MPa√m]	3.85

Table 3. Material properties of the aluminum alloy plate

The panel is subjected to various tests with a sinusoidal uniaxial load at 1 Hz Tables 3 and 4 report the mechanical properties of the aluminium alloy panel and the loading conditions, respectively

Tests	**Load [kN]**	**σ_{max} [MPa]**	**σ_{min} [MPa]**
Test 1	14.71	54.50	0
Test 2	22.07	81.75	0
Test 3	29.43	109.01	0

Table 4. Load conditions applied in the tests

3. Panel without patch

3.1 Analytical procedure

In the present analysis, the Irwin - Westergaard model (Pook, 2000) is used to calculate SIF in the panels without patch. The basic relationships are herein reported. The linear elastic fracture mechanics (LEFM) for a plate of infinite size and central crack (opening mode I) is given by the following expression:

$$K_I = \sigma\sqrt{\pi a} \tag{1}$$

The stress intensity factor, K_I, completely characterizes the stress distribution at the crack tip in a linear elastic material where σ is the asymptotic tensile stress perpendicular to the crack plane and a is the crack half-length. Since the plate is of finite size, the boundary conditions introduce an higher stress intensification at the crack tip. The mode I stress intensity factor is given by (Jukes & Vogwell, 1995; Feddersen, 1996):

$$K_I = \Delta\sigma\sqrt{\pi a}\left[sec\left(\frac{\pi a}{Wp}\right)\right]^{\frac{1}{2}} \tag{2}$$

The elastic stress analysis becomes highly inaccurate as the inelastic region at the crack tip grows up. Simple corrections to the linear elastic fracture mechanics are available when moderate crack tip yielding occurs (Tada et al., 1985; Burdekin & Stone; McClintock & Irwin, 1965). The size of the crack tip yielding zone can be estimated by the Irwin approach, where the elastic stress analysis is used to estimate the elastic plastic boundary. A first order estimation of the plastic zone size, r_y, is

$$r_y = \frac{1}{2\pi}\left(\frac{K_I}{\sigma_s}\right)^2 \tag{3}$$

The stress intensity factor with plasticity correction is given by:

$$K_I^* = \Delta\sigma\sqrt{\pi\left(a - r_y\right)}\left[sec\left(\frac{\pi a}{Wp}\right)\right]^{\frac{1}{2}} \tag{4}$$

The estimation of K_I^*, in Eq.(4), needs an iterative approach.
If this plastic zone is small compared to the crack size, then the linear elastic assumptions are correct. If not, the linear elastic fracture mechanics (LEFM) is not applicable and the elasto-plastic fracture mechanics (EPFM) should be used. The value of K_I^* can be related to G_I, the energy release rate for similar crack growth, in the usual way:

$$K_I^* = \sqrt{G_I E} \tag{5}$$

Where, from the results of Griffith (Griffith, 1924) the energy released normalized with respect to the new crack surface created during the crack extension, namely the strain energy release rate, is given by

$$G_I = -\frac{1}{t_p}\cdot\frac{dU}{da} \tag{6}$$

An increase in the crack length leads to a decrease of the stored elastic strain energy ΔU.

3.2 Numerical procedure

A finite element analysis of the configuration in Fig.1 is carried out, using the finite element code Franc2D/L developed at Kansas University (Swenson & James, 1998).
The plate, without patch, was meshed using standard six node-isoparametric elements with triangular shape, as showed in Fig.2. These elements perform well for elastic analysis and have the advantage that the stress singularity at the crack tip can be incorporated in the solution adopting the quarter-point location method (Henshel & Shaw, 1975). The strain energy release rate is calculated using the modified crack closure method and then the stress intensity factor from the Eq. (5). The values are reported in the Table 5.

For the loading condition #3 the value of K_I^* is close to the fracture toughness. The numerical values are in good agreement with the analytical ones but they are always higher. Fig. 3 presents the comparison between analytical and numerical evaluation of the stress intensity factor as function of the crack length.

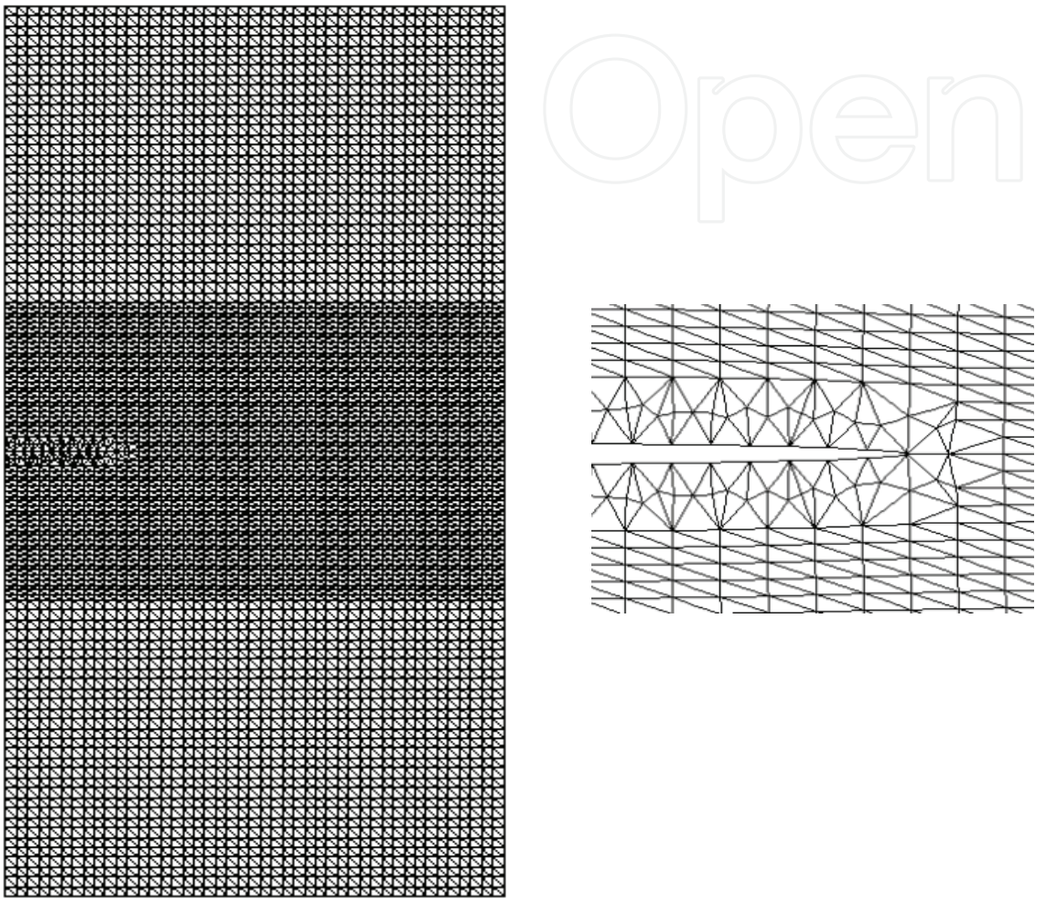

Fig. 2. The finite element model of the half plate geometry: detail of crack tip in pure mode I

The Fig. 3 shows that the good agreement between analytical and numerical results does not depend on the crack length.

	Analytical	**Numerical (FEM)**	**Difference [%]**
Strain Energy Release Rate: G_I [MPa·m]			
Test 1	$2.919 \cdot 10^{-3}$	$3.030 \cdot 10^{-3}$	3.80
Test 2	$6.567 \cdot 10^{-3}$	$6.817 \cdot 10^{-3}$	3.81
Test 3	$1.167 \cdot 10^{-2}$	$1.212 \cdot 10^{-2}$	3.86
SIF: K_I^*[MPa$\sqrt{m}$]			
Test 1	14.23	14.45	1.54
Test 2	21.61	21.68	0.32
Test 3	29.37	28.91	1.57

Table 5. Analytical and numerical values

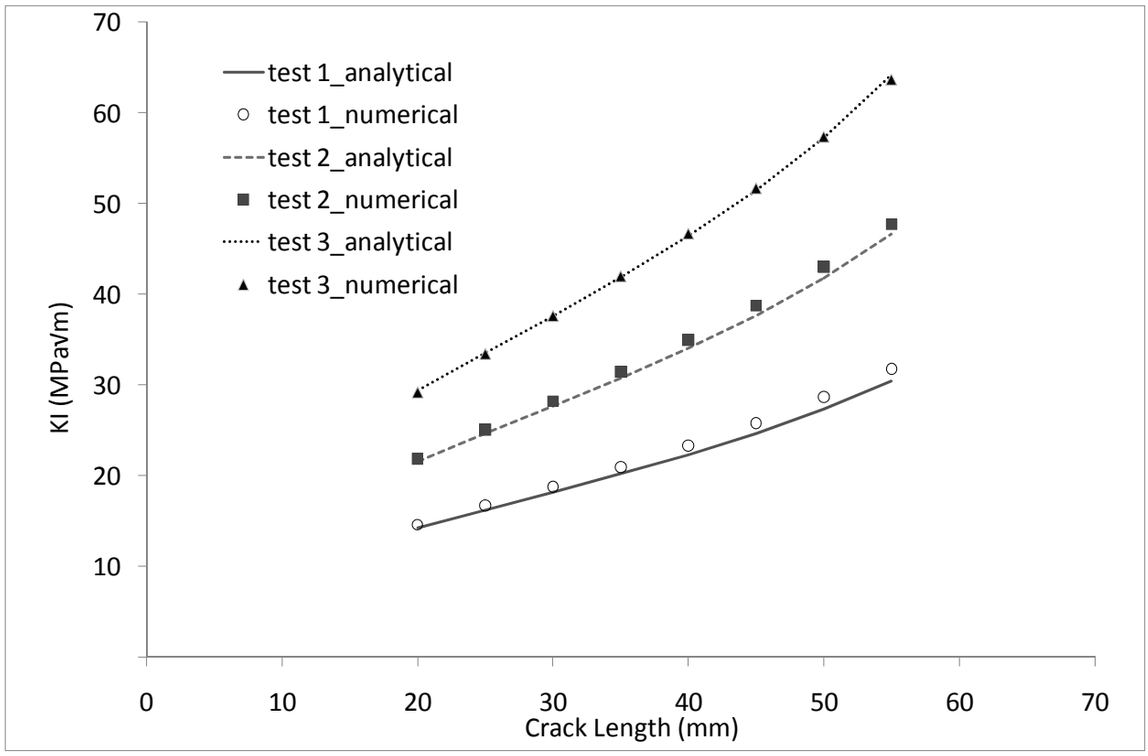

Fig. 3. Analytical and numerical evaluation of the SIF vs. crack length

3.3 Fatigue life prediction

The fatigue-crack growth prediction models usually employ the following Paris power law due to its simplicity (Pook, 2000). In this work, Paris law is used to study the fatigue behaviors of cracked plates:

$$\frac{\mathrm{da}}{\mathrm{dN}} = C(\Delta K)^m \tag{7}$$

The so-called material constants, C and m, for 6061–T6 aluminum alloy, are C=1.8404·10-9, m=2.3. The quantity ΔK is the stress intensity range. Predictions of the fatigue life of plate without patch can be made by numerical solution of the Paris law:

$$\Delta \mathrm{N_i} = \frac{\Delta \mathrm{a_i}}{C(\Delta K_\mathrm{i})^m} \tag{8}$$

where Δa_i is the crack length increment.

The crack grows up in a stable way until the SIF reaches the fracture toughness, i.e. $K_I \geq K_{IC}$. At each calculation step the value of ΔK_i varies due to the crack growth which determines the transformation of the tension state at the crack tip. The loading condition, considered in this study, is characterized by $\sigma_{min} = 0$, with tension ratio $R = 0$, then ΔK_i is simply equal to K_{max}: namely the SIF value corresponding to the K_I^* analytically or numerically calculated.

The value of ΔK_i, is then corrected to take into account two phenomena that affect the rate of the crack growth: the closure of the crack and the static fracture (Pook, 2000).

Aa a crack cannot grow up when it is closed, ΔK becomes:

$$\Delta K_{eff} = K_I^* - K_{th} \tag{9}$$

where K_{th} is the material threshold value.
The crack growth rate depends on the value of ΔK_i which is function itself of the crack length. But the rate of the crack growth increases more rapidly when the critical condition of fracture is reached. In order to model the contribution of the static fracture the Eq. (9) is modified by the term K_{fs}:

$$\Delta K_{eff}{}^* = \Delta K_{eff} + K_{fs} \tag{10}$$

where

$$K_{fs} = \frac{\Delta K_{eff}}{\mathrm{K_{IC}} - \Delta K_{eff}} \tag{11}$$

Obviously the added term K_{fs} becomes more and more dominant as ΔK_{eff} reaches the fracture toughness value.

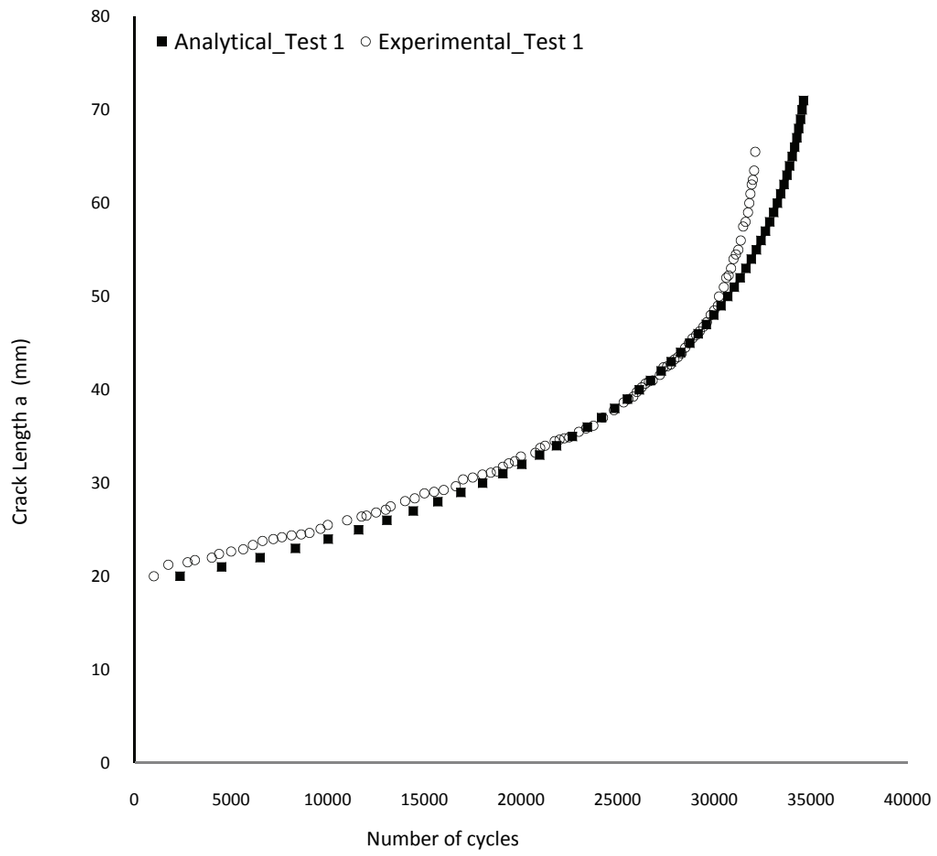

Fig. 3. The experimental and numerical fatigue life for the loading condition "Test 1"

Table 6 shows the analytical results of fatigue tests carried out for the three loading conditions. The number of cycles to failure is based on the K_{max} criterion, i.e.when the K_{max} reaches the fracture toughness K_{IC}

	Load [kN]	Number of cycles to failure
Test 1	14.71	34622
Test 2	22.07	9658
Test 3	29.43	2267

Table 6. Fatigue life prediction of the cracked un-patched panel

The Fig. 3 shows a comparison of the crack growth between the numerical model (Eqns. 7-11) and the experimental results for the cracked panel (without patch) under the loading condition #1. The details of the experimental measurements are reported in Section 5. The higher experimental crack growth rate at the number of cycles close to the failure is due to an asymmetric growth of the crack experienced during the tests.

4. Panel with patch

4.1 Analytical procedure

Rose's analytical model (Rose, 1981 and 1982) is used to compute the SIF for the repaired plates by single patch,

$$K_R = Y \cdot \sigma_0 / \sqrt{\mathrm{k}} \tag{12}$$

where Y is a geometric factor, which accounts for repairs to center or edge cracks; Y=1 for a repair to a centre crack; σ_0 is the nominal stress that would exist in an uncracked plate after the application of a patch:

$$\sigma_0 = \frac{\Delta\sigma}{1+S} \tag{13}$$

where $S=E_r t_r / E_p t_p$. k represents a spring constant given by:

$$\mathrm{k} = \frac{\beta S}{(1+S)(1-\nu_p)} \tag{14}$$

where β is a shear stress transfer length in a representative bonded joint:

$$\beta = \left[\frac{G_a}{t_a}\left(\frac{1}{E_p t_p} + \frac{1}{E_r t_r}\right)\right]^{\frac{1}{2}} \tag{15}$$

In the case of one sided repairs, Ratwani (Ratwani, 1979) provided a bending correction factor:

$$K_R^* = (1 + BC) K_R \tag{16}$$

where K^*_R is the stress intensity factor for a one sided repair, the correction term BC is given by:

$$BC = a y_{max} \left(1 - \frac{K_R}{K_I^*}\right) \frac{t_p (t_p + t_r)}{I} \tag{17}$$

where y_{max} is the distance of the extreme fiber ply from the neutral axis of the cracked plate:

$$y_{max} = t_p + Z \tag{18}$$

with

$$Z = \frac{S(t_p+t_r+2t_a)}{2(1+S)} \tag{19}$$

and I is the total moment of inertia of the plate repair:

$$I = I_p + nI_r \qquad and \quad n = \frac{E_r}{E_p} \tag{20}$$

where

$$I_p = w_p \frac{t_p^3}{12} + w_p t_p Z^2 \tag{21}$$

$$I_r = w_r \frac{t_r^3}{12} + w_r t_r \frac{\left[\frac{t_r}{2} + t_a + (\frac{t_p}{2} - Z)\right]^2}{4} \tag{22}$$

The stress intensity factors, computed with the above mentioned analytical procedure, for the different patch configurations (i.e. fiber lay-up and adhesive type) are shown in the Tables 7.

Specimen Configuration	**Analytical K^*_R [MPa√m]**	**FEM K^*_R [MPa√m]**	**Difference [%]**
Test 1 - repaired plate:			
patch type 1 + ad. EA956	8.62	8.32	-3.6
patch type 1 + ad. FM73	8.97	9.22	2.6
patch type 1 + ad. AF163-2K	9.12	9.54	4.4
patch type 2 + ad. EA956	10.15	9.95	-2.0
patch type 2 + ad. FM73	10.4	10.91	4.7
patch type 2 + ad. AF163-2K	10.5	11.24	6.6

Table 7.1. Analytical and numerical SIF for the repaired plate in Test 1

Test 2 - repaired plate:			
patch type 1 + ad. EA956	12.92	12.51	-3.3
patch type 1 + ad. FM73	13.46	13.87	2.9
patch type 1 + ad. AF163-2K	13.67	14.35	4.7
patch type 2 + ad. EA956	15.23	14.98	-1.7
patch type 2 + ad. FM73	15.59	16.43	5.1
patch type 2 + ad. AF163-2K	15.75	16.94	7.0

Table 7.2. Analytical and numerical SIF for the repaired plate in Test 2

Test 3 - repaired plate:			
patch type 1 + ad. EA956	17.23	16.75	-2.9
patch type 1 + ad. FM73	17.95	18.58	3.4
patch type 1 + ad. AF163-2K	18.23	19.23	5.2
patch type 2 + ad. EA956	20.3	20.08	-1.1
patch type 2 + ad. FM73	20.8	22.15	6.1
patch type 2 + ad. AF163-2K	21.0	22.74	7.6

Table 7.3. Analytical and numerical SIF for the repaired plate in Test 3

4.2 Numerical procedure

A finite element analysis of the configurations of Fig. 4 is carried out using the finite element code Franc2D/L for the total structure (plate and patch).

The patched plate is meshed using standard two-dimensional six node isoparametric elements with triangular shape.

The repaired structure is modeled as three layer structure (plate, patch and adhesive). Due to the symmetry of the problem, only half plate is modeled using 29373 nodes and 14578 elements. Tables from 7.1 to 7.3 report the SIF obtained with the finite element models and the comparison with the previous analytical results. The configuration with the adhesive AF163-2K usually demonstrates the highest difference between numerical and analytical values. This performance is due to improved atomic bond of the glue. The adhesive AF163-2K has the lowest elastic and shear moduli. The patch type 2 always provides a higher SIF and among these configurations those using the adhesive AF163-2K are the highest.

5. Experimental procedure

5.1 Testing procedure

In order to verify the effectiveness of analytical and numerical analyses some experimental measurements, for the damaged and repaired panels, are carried out. The tests are performed at room temperature in a 100 kN Metrocom Engineering SpA servo-hydraulic test machine. The tests are focused to evaluate the fatigue life of the structures under cycling loads at R=0 as described in Section 2 – Table 4. Each test is performed up to the complete fracture of the panel. In each test the number of the cycles, the crack growth and the SIF are evaluated. In particular the SIF is measured at the crack tip using three measurement grids strain-gauges. A National Instrument data acquisition system is used to acquire the load and strain measurements during the tests.

In all the experimental tests the panel surface is treated with a solvent to clean and remove any impurities and / or contamination from the surface and subjected to a local mechanical abrasion to increase and activate the contact surfaces between the metal panel and the composite patch. In the configuration A4 reported in the Table 8, the surface is subjected to a treatment of pickling sulfur chromium for aluminum alloys according to UNI EN 2334:1998 - Aerospace Division.

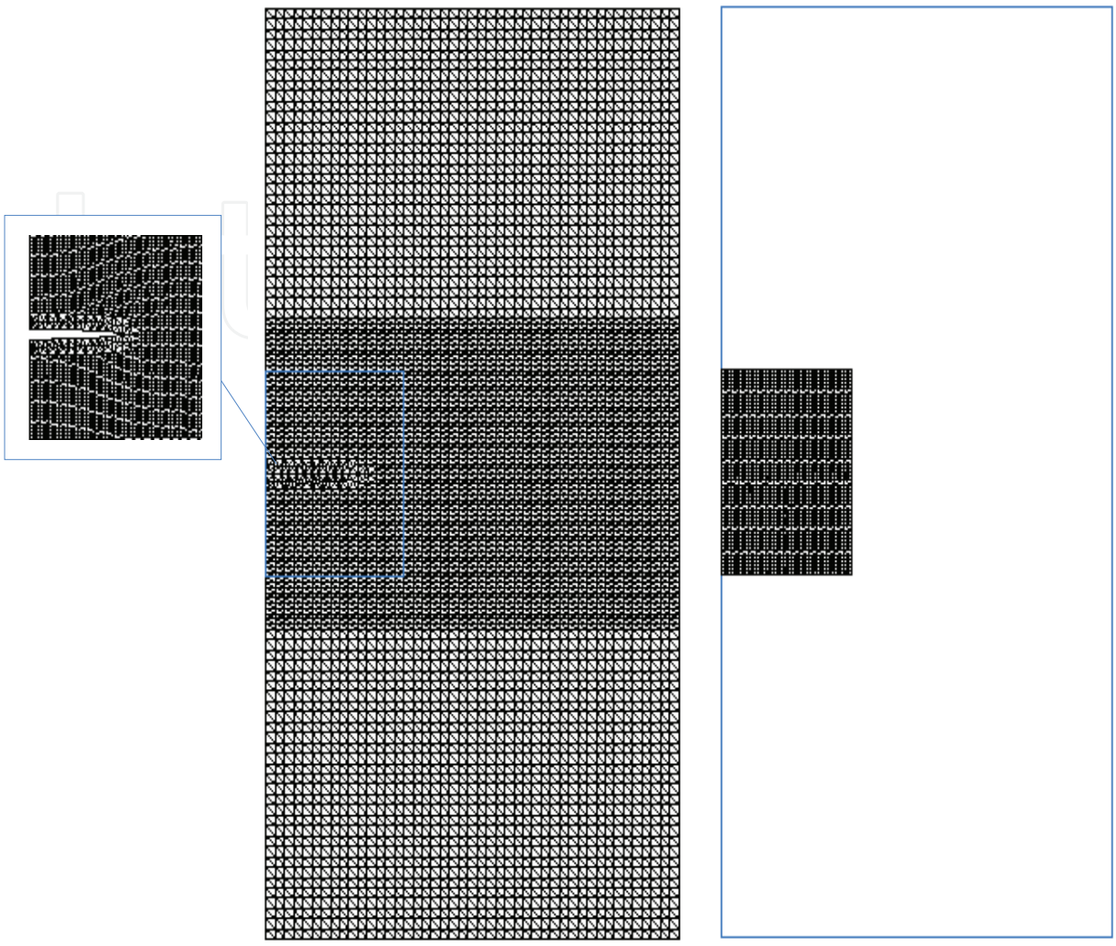

Fig. 4. Finite element model of the plate repaired with the composite patch

5.2 Experimental results

Among all the possible combinations of patch and adhesive types and loading conditions, a subset of tests is carried out. The experimental configurations, discussed in the present work, are summarized in Table 8:

Configuration Name	Patch Type	Adhesive Type	Loading Condition	Surface Treatment
A1	Type 1	EA956	Test 2	Yes
A2	Type 2	FM 73	Test 2	Yes
A3	Type 2	AF163-2K	Test 2	Yes
A4	Type 2	AF163-2K	Test 2	Yes
B1	Type 1	EA956	Test 3	Yes
B2	Type 1	EA956	Test 3	Yes

Table 8. Experimental configurations

A good repeatability is found for the configurations A1÷A4 as the load amplitude is a moderate percentage of the ultimate static load. The configurations B1 e B2 are characterized by an higher load amplitudes. Moreover for the configuration B1 the patch is bonded using the technique of mechanical compression; on the contrary for the configuration B2 it is bonded using the vacuum bag technique. Therefore the results of the configurations B1 and B2 are presented separately in order to show the scatter of the experimental results, summarized in the Tables 9 and 10. The configurations A1 showed the best performances in terms of stress level and fatigue life. The configuration A1 is repaired with a patch "Type 1" that is thicker and therefore introduces a higher stiffness by increasing the fatigue life, but amplifies the bending in the panel. The configurations A2÷A4, with the same type of bonded patch, show the role of both the adhesive layer and the surface treatment. In particular the configuration A4 provides a fatigue life comparable with configuration A1 although the measured SIF for A4 is the highest among the configurations A. In Fig. 5 it is shown how for the configuration A4 the crack propagates through the composite patch leading to the simultaneous fracture of the metal panel and of the patch.
In other configurations the crack propagates in the adhesive layer and the patch slid over the panel surface as showed in Fig. 6.

Configuration Name	**Experimental**	**Numerical**	**Difference [%]**
A1	13.61	12.92	5.1
A2	14.85	15.59	-5.0
A3	15.11	15.75	-4.3
A4	16.83	15.75	6.4
B1	17.89	17.36	3.0
B2	18.02	17.36	3.7

Table 9. SIF - K_I [MPa√m]: Experimental and numerical results

Configuration Name	**Experimental**	**Numerical**	**Difference [%]**
A1	21770	23188	-6.51
A2	18843	21207	-12.50
A3	19375	21268	-9.77
A4	21450	21268	0.85
B1	4425	5235	-18.30
B2	4926	5235	-6.27

Table 10. Fatigue cycles: Experimental and numerical results

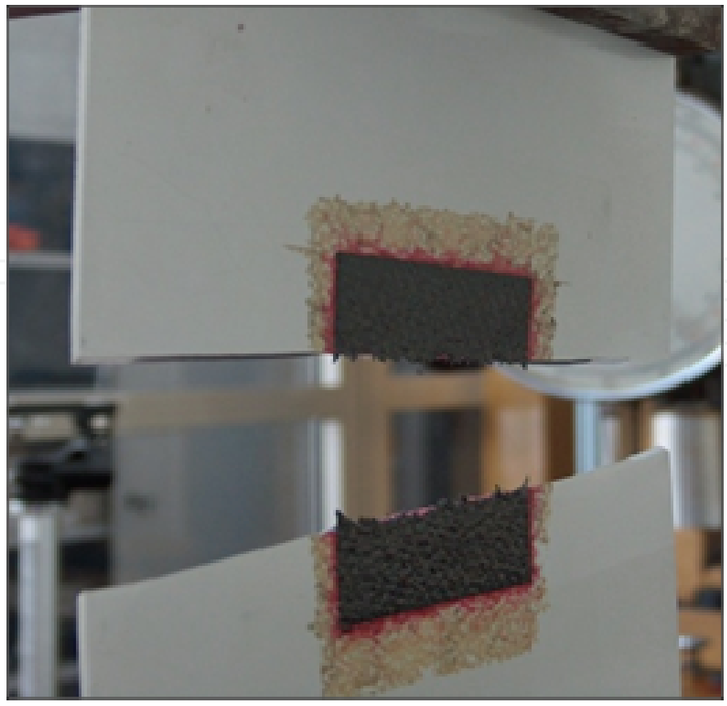

Fig. 5. The configuration A4: the crack propagated through the composite patch

Fig. 6. The crack propagated in the adhesive layer that leads to the sliding of the full patch

The configurations B demonstrate again the role of the curing procedure and a small variation in the SIF provided a larger difference in the fatigue life.

5.3 Comparison of numerical and experimental results

The developed finite element models are not able to take account of the difference between the configurations A3, A4 and B1, B2. Therefore the same numerical value is reported in the Tables 9 and 10. The comparison of the SIF shows a good agreement between experimental and numerical results. On the contrary, the numerical results, in general, overestimated the experimental fatigue life. The small differences in terms of SIF values lead to a larger overestimation of the fatigue life. The curing procedure of the patch on the metallic panel introduces random factors that cannot be easily accounted for in the finite element model reducing its predictive capabilities.

6. Final considerations and conclusions

The main purpose of this study has been the determination of the effectiveness of bonded composite patches to repair cracked thin aluminum panels. The repair is realized by patching only one side of the panel in order to reduce the associated costs and time required. In most of the cases, in fact, the other side of the panels is not easily accessible. Moreover, this type of repair might be applied locally without the need of disassembling a complex structure.

Several experimental tests are carried out to obtain a set of data useful to estimate the state of stress and the fatigue behavior of cracked and bonded repaired panels and to define the effectiveness of the repairing patch. The comparison of the data obtained from the cracked and patch repaired panels have pointed out a significative reduction of the stress intensity factor at the crack tips in the repaired configurations. The experimental tests demonstrate a reduction of the average stress of about 30% due to the patch that turns out in an increase of about 50% of the fatigue life. To support the experimental activities and reduce the associated costs, theoretical and numerical models have been developed and the mechanisms of the damage propagation by using fracture mechanics and fatigue strength analyzed.

The capabilities of numerical and analytical methods are compared with a set of experimental results. In particular the analytical model, based on Rose's analytical solution and Paris' law, are developed to predict the stress intensity factor and the fatigue life of the panel with and without repair.

The numerical and experimental results show that the bonded patch highly reduces the stress intensity factor and increases the fatigue life. Moreover, it has been shown that the effectiveness of the repair strongly depends on the patch stiffness, adhesive characteristics, surface treatments and in general curing procedure. The effectiveness of the composite patches is shown in the next results.

The SIF values, evaluated with the Franc2D/L finite element code and reported in Table 12, show the benefits of the patch repair due to a decrease of about 30% of the stress amplitude near the crack tips.

Specimen Configuration	**Load [kN]**	**K_I(MPa√m)**	**K_I(MPa√m)**	**Difference [%]**
		(Average Value Experimental)		
		Without Patch	*With Patch*	
Test 1	14.71	14.23	9.61	32.5
Test 2	22.07	21.62	14.46	33.1
Test 3	29.43	29.37	19.38	34.0

Table 12. Comparison of the panel with and without patch

The Fig. 7 shows how the SIF as function of the crack length is attenuated when the through thickness cracked plate is repaired with a bonded patch (Test 2). The finite element model takes into account a progressive patch cracking as far as the crack grows up in the plate, even though the effect of the patch, including the SIF growth rate, might be different as explained in the Section 5.2. When the crack tips overtake the edges of the patch, the crack growth rate quickly increases as showed in Fig. 8. In this figure the crack length is plotted as function of the number of loading cycles for the patched and unpatched aluminum cracked plate used in the experiments (Test 2). For the patched panel, it is evident as the growth rate increases when the crack becomes larger than the patch width. Table 13 summarizes the fatigue lifes for various specimen configurations.
The fatigue life of the repaired plate increases of about 110%. The bonded patch can significantly increase the fatigue life of the cracked panel, depending on the stiffness of the patch, the adhesive characteristics, the surface treatments and, in general, the procedure used to apply the patch.

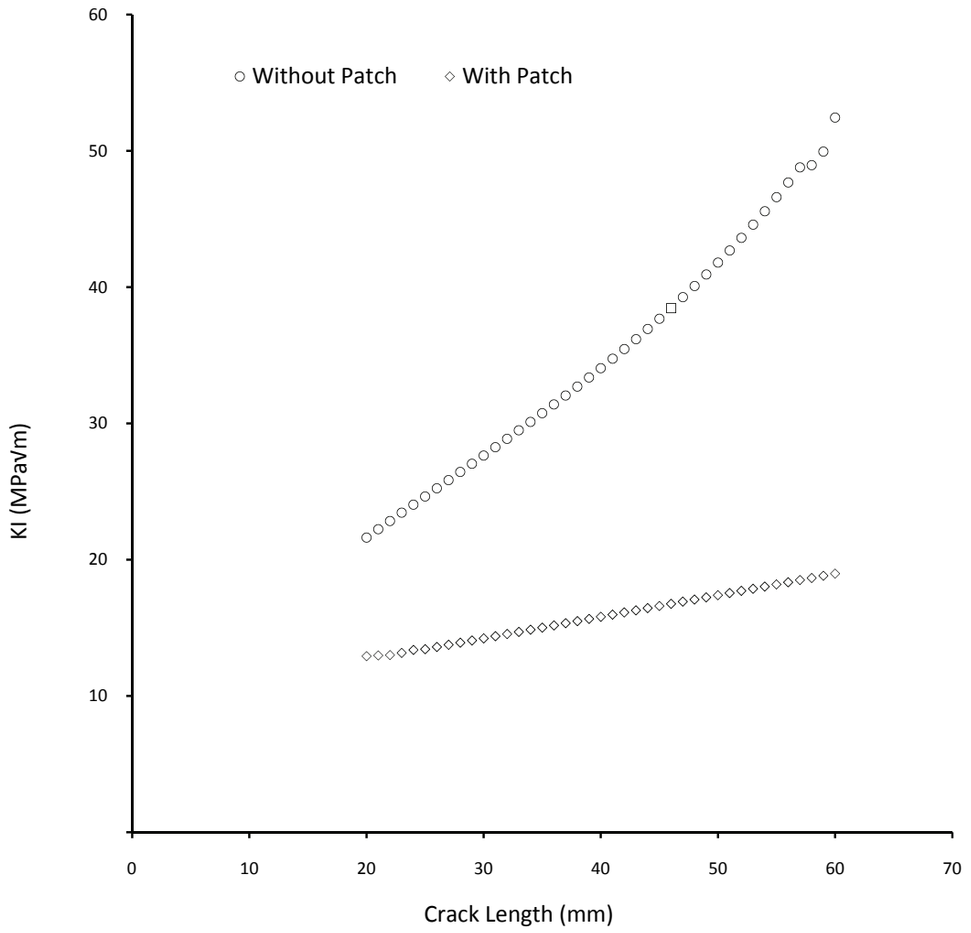

Fig. 7. Comparison of the SIF between patched (test 2 plate repaired A1) and unpatched cracks

Specimen Configuration	Load [kN]	Fatigue life Cycles *(Average Value Experimental)*	Fatigue life Cycles	Difference [%]
		Without Patch	*With Patch*	
Test 1	14.71	34622	72628	-109
Test 2	22.07	9658	20354	-110
Test 3	29.43	2267	4675	-106

Table 13. Comparison of the fatigue life of the panel with and without patch

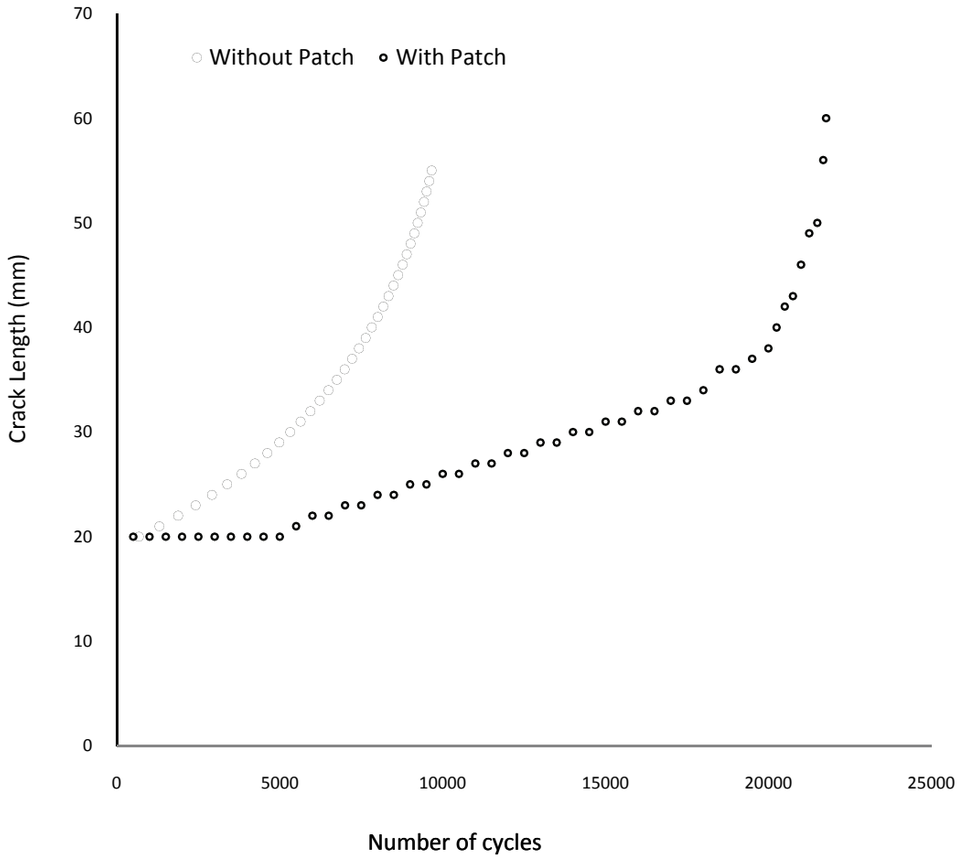

Fig. 8. Comparison the crack length vs. loading cycles

7. References

Baker A.A. & Jones R. (1987). *Bonded repair of aircraft structures*, Martinus Nijhoff, ISBN: 90-247-3606-4, The Netherlands

Pook L.P. (2000). *Linear Elastic Fracture Mechanics for Engineers: Theory and Applications*. WITPRESS, ISBN:1 8531 2703 5, Computational Mechanics Inc.

Swenson D. & James M. (1997). *FRANC2D/L: A crack propagation simulator for plane layered structures*. Version 1.4, User's Guide, University of Kansas, USA

Tada H., Paris P.C., Irwin G.R. (1985). *Handbook of the stress analysis of cracks*, Paris Productions Incorporated, St. Louis, Missouri, USA

Roach D. (1995). Performance analysis of bonded composite doublers on aircraft structures, *International Conference on Composite repair of aircraft,* (08/1995), Vancouver, Canada

Tong L. & Sun X. (2003). Nonlinear stress analysis for bonded patch to curved thin-walled structures, International Journal of Adhesion & Adhesives, Vol. 23, No. 5, pp. 349-364

Baker A.A.; Callinan R.J.; Davis M.J.; Jones R. & Williams J.G. (1984). Repair of Mirage III aircraft using BFRP crack patching technology, *Theoretical and Applied Fracture Mechanics*, Vol. 2, No.1, (10/1984), page numbers (1-16)

Baker A.A. (1993). Repair efficiency in fatigued-cracked aluminum components reinforced with boron/epoxy patches. *Fatigue and Fracture of Engineering Materials and Structures*, Vol. 16, No. 7, (07/1993), page numbers (753-765), ISSN: 8756-758X

Burdekin F.M. & Stone D.E.W. (1966). The crack opening displacement approach to fracture mechanics in yielding materials. *Journal of Strain Analysis*, Vol. 1 , page numbers (145-153)

Christian T.F. Jr.; Hammond D.O. & Cochran J.B.(1992). Composite material repairs to metallic airframe components, *Journal Aircraft*, Vol. 29, page numbers (470–476)

Chung H.K. & Yang W.H. (2002). Fracture mechanics analysis on the bonded repair of a skin/stiffener with an inclined central crack, *Composite Structures*, Vol. 55, No. 3, (02/2002), page numbers (269-276)

Griffith A.A. (1921). The phenomenon of rupture and flow in solids. *Philosophical Transsactions of the Royal Society of London*, Series A, Vol.221, page numbers (163-198)

Henshel R.D. & Shaw K.G. (1975). Crack tip finite elements are unnecessary. *International Journal for Numerical Methods in Engineering,* Vol.9, No.3, page numbers (495–507)

Jones R.; Whittingham B. & Marshall I.H. (2002). Bonded repairs to rib stiffened wing skins, *Composite Structures*, Vol.57, No. 1, page numbers (453-458)

Jukes R. & Vogwell J. (1995). A method for establishing geometry correction factors by ratio of finite element stresses, Engineering fracture mechanics, Vol. 50, No. 4, page numbers (581-589)

Klug J.C.; Maley S. & Sun C.T. (1999). Characterization of fatigue behavior of bonded composite repairs, *Journal Aircraf,* Vol. 36, No. 6, page numbers (1016-1022)

Mahadesh Kumar A. & Hakeem S.A. (2000). Optimum design of symmetric composite patch repair to centre cracked metallic sheet, *Composite Structures*, Vol. 49, No. 3, (07/2000), page numbers (285-292)

Molent L.;Callinan R.J. & Jones R. (1989). Structural aspects of the design of an all boron/epoxy reinforcement for the F-l 11C wing pivot fitting, *Composite Structures,* Vol. 11, page numbers (57-83)

Naboulsi S. & Mall S. (1996). Modeling of a cracked metallic structure with bonded composite patch using the three layer technique, *Composite Structures*, Vol. 35, page numbers (295-308)

Naboulsi S. & Mall S. (1998). Nonlinear analysis of bonded composite patch repair of cracked aluminum panels, *Composite Structures*, Vol. 41, page numbers (303-313)

Ratwani M.M. (1979). Analysis of Cracked, Adhesively Bonded Laminated Structures. *AIAA Journal,* Vol. 17, No. 9, (09/1979), page numbers (988-994)

Rose L.R.F. (1981). An application of the inclusion analogy for bonded reinforcements. *International Journal Solid Structure*, Vol. 17, No. 8, page numbers (827–838)

Rose L.R.F. (1982). A cracked plate repaired with bonded reinforcements, *International Journal of Fracture*, Vol. 18, No. 2, (02/1982), page numbers (135-144)

Schubbe J.J. & Mall S. (1999). Modeling of cracked thick metallic structure with bonded composite patch repair using three-layer technique, *Composite Structures*, Vol. 45, No.3, (06/1999), page numbers (185-193)

Schubbe J.J. & Mall S. (1999). Investigation of cracked aluminium panel repaired with bonded composite patch, *Engineering Fracture Mechanics,* Vol. 63, No. 3, (06/1999), page numbers (305-323)

Umamaheswar T.V.R.S. & Singh R. (1999). Modeling of a patch repair to a thin cracked sheet. *Engineering Fracture Mechanics, Vol*. 62, page numbers (267–289)

Wang J.; Rider A. N.; Heller M. & Kaye M. (2005). Theoretical and experimental research into optimal edge taper of bonded repair patches subject to fatigue loadings. *International of Adhesion & Adhesives*, Vol. 25, page numbers (410-426)

Bartholomeus R.A.; Paul J.J. & Roberts J.D. (1991). Application of bonded composite repair technology to Civilian Aircraft - 747 Demonstrator Program, In: *National Conference Publication on Aircraft Damage Assessment and Repair,* Institution of Engineers, (91 pt 17), page numbers (216-220), ISBN 85825 537 5, Australia

Feddersen C.E (1966). Plane strain crack toughness testing of high strength metallic materials, In: *W.F. Brown and J.E. Srawley*, ASTM STP 410, page numbers (77-79)

McClintock F.A. & Irwin G.R. (1965). Plasticity Aspects of Fracture Mechanics, In: *Fracture toughness testing and its applications*, ASTM STP 381, page numbers (84-113), ISBN-EB: 978-0-8031-4569-6

Torkington C. (1991). The regulatory aspects of the repair of civil aircraft metal structures, In: *International Conference on Aircraft Damage Assessment and Repair,* Institution of Engineers, page numbers (1-5), ISBN: 0858255375, Melbourne Victoria, Australia

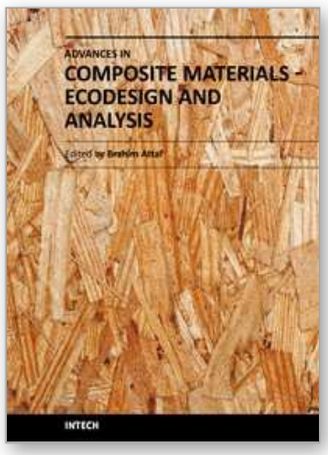

Advances in Composite Materials - Ecodesign and Analysis
Edited by Dr. Brahim Attaf

ISBN 978-953-307-150-3
Hard cover, 642 pages
Publisher InTech
Published online 16, March, 2011
Published in print edition March, 2011

By adopting the principles of sustainable design and cleaner production, this important book opens a new challenge in the world of composite materials and explores the achieved advancements of specialists in their respective areas of research and innovation. Contributions coming from both spaces of academia and industry were so diversified that the 28 chapters composing the book have been grouped into the following main parts: sustainable materials and ecodesign aspects, composite materials and curing processes, modelling and testing, strength of adhesive joints, characterization and thermal behaviour, all of which provides an invaluable overview of this fascinating subject area. Results achieved from theoretical, numerical and experimental investigations can help designers, manufacturers and suppliers involved with high-tech composite materials to boost competitiveness and innovation productivity.

INTECH
open science | open minds

InTech Europe
University Campus STeP Ri
Slavka Krautzeka 83/A
51000 Rijeka, Croatia
Phone: +385 (51) 770 447
Fax: +385 (51) 686 166
www.intechopen.com

InTech China
Unit 405, Office Block, Hotel Equatorial Shanghai
No.65, Yan An Road (West), Shanghai, 200040, China
中国上海市延安西路65号上海国际贵都大饭店办公楼405单元
Phone: +86-21-62489820
Fax: +86-21-62489821

IntechOpen